Effects of the Anode Diffusion Layer on the Performance of a Nonenzymatic Electrochemical Glucose Fuel Cell with a Proton Exchange Membrane

Hyeonjin Cha, Obeen Kwon, Jaeyeon Kim, Heesoo Choi, Hongnyoung Yoo, Hyeok Kim, and Taehyun Park*

Read Online

ACCESS | 📊 Metrics & More | 📰 Article Recommendations

ABSTRACT: It is necessary to apply a nonenzymatic glucose fuel cell using a proton exchange membrane for an implantable biomedical device that operates at low power. The permeability of glucose with high viscosity and a large molecular weight in the porous medium of the diffusion layer was investigated for use in fuel cells. Carbon paper was prepared as an anode diffusion layer, and it was analyzed with a diffusion layer treated with polytetrafluoroethylene (PTFE) and a microporous layer (MPL). When untreated carbon paper was applied, the peak power density (PPD) and open-circuit voltage (OCV) increased as the glucose concentration and flow rate increased. On this occasion, the highest PPD of 17.81 μW cm^{-2} was achieved at 3 mM and a 2.0 mL min^{-1} glucose aqueous solution (at atmospheric pressure and 36.5 °C). The diffusion layer, which became more hydrophobic through PTFE treatment, adversely affected glucose permeability. In addition, the addition of an MPL decreased OCV and PPD with increasing glucose concentrations and flow rates. Compared with untreated carbon paper, the PPD was six times lower approximately. Consequently, it was confirmed that the properties of carbon paper, such as low hydrophobicity, high porosity, and thin thickness, would be advantageous for nonenzymatic glucose fuel cells.
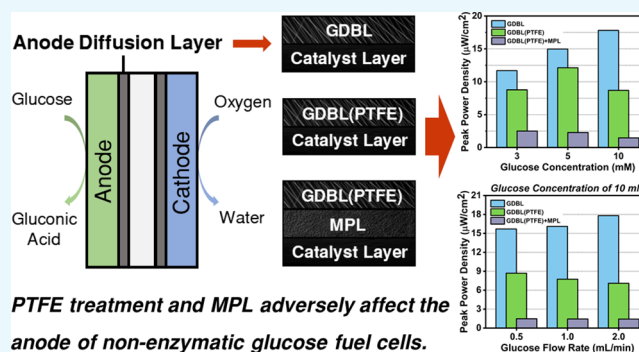
INTRODUCTION

Glucose is the most abundant monosaccharide in nature and is a renewable energy source. In recent years, glucose has been explored for various applications in the medical field owing to its advantages, such as eco-friendliness, availability, and biocompatibility compared to conventional batteries.[1−5] Glucose has a lower energy density per weight than hydrogen but has a theoretical energy density (4430 Wh kg^{-1}) of the same order of magnitude as methanol (6100 Wh kg^{-1}).[6−9] Therefore, compared to hydrogen production and its storage difficulties, using glucose as a fuel may reduce production and management costs. In addition, glucose is an endogenous compound in body fluids with low toxicity and good biocompatibility.[10,11] Accordingly, glucose in the body's blood can be used as an electrochemical energy source, and it opens the possibility of using oxygen dissolved in body fluids for implantable fuel cells. Lithium iodine batteries are the primary power source for implantable medical devices and pacemakers.[12−14] However, because more than half of all pacemakers end their life after 5−8 years because of the depletion of the charged electrical energy in the battery, the patient must periodically undergo surgery to replace the exhausted battery.[15,16] Thus, if a high-durability fuel cell that

uses glucose in the body as an energy source to generate electric power to drive an implantable device is used, this problem can be solved with a semipermanent power source when implanted in the body. Furthermore, glucose can be used as an electrochemical sensor. It is fast, accurate, and sensitive.[17,18] Thus, if glucose is used as a biosensor, then blood glucose can be measured in real time through electrochemical sensing, and a quick response is possible.

An enzymatic fuel cell using enzymes as anode catalysts generates 24 electrons and CO$_2$ through complete oxidation in the decomposition reaction of glucose.[19] They use glucose oxidase or glucose dehydrogenase as enzymes and generate several mW cm^{-2} through high catalytic efficiency in glucose oxidation.[16,20−23] However, enzyme-based fuel cells have a short operating life span because of enzyme instability.[9,16,24]

When used for a long time, the complex protein structure of the enzyme is degraded and gradually inactivated.[21] In contrast, a nonenzymatic glucose fuel cell uses abiotic catalysts. The catalyst uses noble metals or alloys to promote the oxidation of glucose.[10,21,25] In implantable fuel cells, catalysts can be selected for appropriate biocompatibility.[15,20] Long-term stability is good compared to that of enzymatic fuel cells, so a nonenzymatic glucose fuel cell has excellent durability.[16,21] Also, it is advantageous in terms of mass production because it is simple and easy to handle. Along with the advantages of nonenzymatic glucose fuel cells, there are still problems to be solved. In particular, if the internal structure, characteristics, and conditions are optimized, then the stability part should also be studied.

Figure 1 shows the reaction scheme of a nonenzymatic glucose fuel cell that directly oxidizes glucose using a platinum-
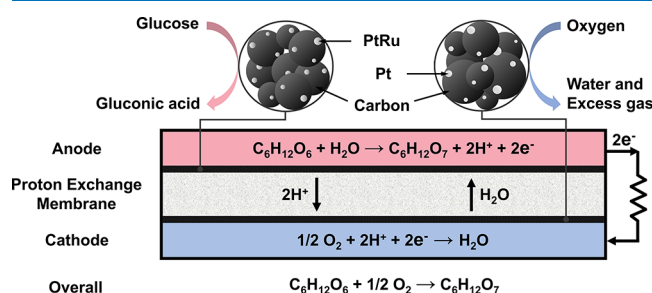

Figure 1. Reaction of a nonenzymatic glucose fuel cell using platinum as a noble metal catalyst in a proton exchange membrane. Using a platinum catalyst, glucose is oxidized directly to glucose acid, and oxygen is reduced to water.

based catalyst in the proton exchange membrane (PEM) used in this experiment. In an alkaline medium supplied with a strong alkaline solution and an anion exchange membrane (AEM), glucose is oxidized more easily, and higher performance can be achieved.[9,21,26,27] However, because the pH of body fluids containing glucose cannot be alkaline, it cannot be used in implantable medical device applications. Theoretically, the glucose oxidation reaction (GOR) releases 24 electrons for each glucose molecule in reaction with water.[28−30] However, the poisoning of anode catalysts by intermediate oxides and the slow electrochemical kinetics of glucose oxidation are significant obstacles.[31−35] Due to the difficulty of glucose oxidation, most of the glucose ($C_6H_{12}O_6$) is oxidized to gluconic acid ($C_6H_{12}O_7$) and emits two electrons.[10,36,37] This limits the performance of the glucose fuel cell to levels considerably lower than the theoretical energy density.[10,38]

Despite the promising results of glucose fuel cells, efforts are underway to improve the efficiency and performance of electro-oxidation. This promotes glucose oxidation by using a metal nanoparticle-based catalyst, preventing poisoning of intermediate products and reducing long-term loss. Platinum is the best catalyst for the electrical oxidation of glucose.[27,30,32,39] However, platinum poisoning occurs as the absorption of intermediates such as gluconic acid continues during glucose oxidation, especially at high glucose concentrations.[21,40,41] A bimetallic alloy catalyst using Au, Ru, Pd, and Bi based on platinum has been reported.[38,42−44] Also, there are studies on electrodes or modified carbon-based materials such as carbon nanotubes or graphene oxide used as catalyst supports. Li et al.[45] reduced the layer by stacking a Pd-based nanocatalyst on carbon foam with a large specific area. Song et al.[29]

investigated the polytetrafluoroethylene (PTFE) content, the carbon content, the anode catalyst loading amount, and the binder type of the anode MPL in AEM glucose fuel cells. Zhao et al.[46] reported that a hydrophobic layer added to the cathode facilitates water transportation in alkaline liquid fuel. The effect of the content and the type of carbon material in the microporous layer (MPL) on the cathode potential was analyzed. A glucose fuel cell using an AEM requires a strongly basic aqueous solution such as KOH, and water is produced at the anode. However, corrosion of the diffusion layer may be accelerated by strong basicity and may be excluded when considering insertion into the body. On the other hand, in the glucose fuel cell using a PEM, water is generated at the cathode, and the glucose solution injected into the anode is composed of pure water. Therefore, changing the properties of the diffusion layer is meaningful in terms of water management and permeability. However, a review of extant studies indicates few studies related to the effect of the anode diffusion layer characteristics of nonenzymatic glucose fuel cells on the performance.

In this study, the effect of changes in the glucose concentration and flow rate on the performance of nonenzymatic glucose fuel cells was analyzed. To confirm the feasibility, the trend at the anode was investigated by applying the gas diffusion layer used in general proton exchange membrane fuel cells (PEMFCs). Based on the carbon paper-based diffusion layer, the overall trend and performance were compared through a total of three cases: a diffusion layer without any treatment, with PTFE treatment only, or with PTFE and an MPL added.

■ RESULTS AND DISCUSSION

This experiment demonstrates a nonenzymatic glucose fuel cell that directly oxidizes glucose through a platinum-based catalyst. The glucose oxidation reaction (GOR) kinetics are considerably slower than those of the oxygen reduction reaction (ORR) in glucose fuel cells. Therefore, the current generated by the electrochemical reaction is dependent on the glucose reaction due to the rate-determining step (RDS) by the kinetics.[47] Owing to the extremely high anodic activation loss, the actual current density generated by the electrochemical reaction is inevitably low.[48] Unlike fuel cells that use available hydrogen and oxygen, anodic activation loss is more dominant in glucose fuel cells than in the cathode, so a high catalyst amount is required to reduce this loss.[49] As a result, more glucose must react in the catalyst layer. Therefore, the Pt catalyst loading content in this experiment was fixed at 1.0 mg cm^{-2}. The specific catalyst loading content used in conventional abiotic glucose fuel cells is 2.0−4.0 mg cm^{-2}.[8,27,50] To analyze the change according to the characteristics of the diffusion layer in a nonenzymatic glucose fuel cell environment, the concentration and flow rate of glucose were set as important variables. Table 1 lists the material properties of the carbon paper used as the GDL of the anode.[51,52] It shows the characteristics of an existing carbon paper-based GDBL (CP_AA), a hydrophobic PTFE-treated GDL (CP_BA), and a both PTFE-treated and MPL-coated GDL (CP_BC).

Effects of Untreated Carbon Paper on Glucose Permeability. Figures 2−4 show the polarization curve and power density according to glucose concentration and flow rate changes when three different anode diffusion layers are used. OCV is theoretically calculated by the Nernst equation. In the Nernst equation, the reversible cell voltage is the standard-state

Table 1. Properties of Materials Applied as a Diffusion Layer of an Anode in This Study[a]

GDL	PTFE treatment	MPL	porosity	thickness (μm)	electrical resistivity ($m\Omega$ cm^2)
CP_AA[a]	no	no	0.88	190	<5
CP_BA[b]	yes	no	0.81	200	<6
CP_BC[c]	yes	yes	0.40	235	<10

[a]Commercially available GDLs (Sigracet Carbon, Ltd., Germany): [a]29AA, [b]29BA, and [c]29BC.

reversible voltage minus the terms of the main variables. In particular, when the concentration of the reactant increases, the reversible voltage increases, which leads to the improvement of PPD and OCV. This is because the thermodynamic reversible voltage is determined according to the concentrations of reactants and products at the reaction site.[53] It is possible to understand the change in OCV according to the concentration of glucose, and it is related to the permeability according to the characteristics of the diffusion layer. However, compared with the theoretical reversible voltage, the OCV of a glucose fuel cell is extremely low. This is because of water crossovers from the anode to the cathode, similar to methanol, as the GOR at the cathode interferes with the ORR to generate a mixed potential.[26] However, because the molecular size of glucose is significantly larger than that of methanol, the crossover may be limited, and this effect will be insignificant.[8,21] Instead, it appears that the difficulty of polarization

due to low catalyst activity plays a more prominent role. Finally, it can be observed that glucose oxidation is not straightforward with a general Pt-based catalyst.

Based on the kinetics, the relationship between the electric current generated in the electrochemical reaction of the fuel cell and the internal loss voltage required to overcome the activation barrier is expressed by the following Butler–Volmer equation:

$$j = j_0^0\left(\frac{C_R^*}{C_R^{0*}}e^{\alpha nF\eta/(RT)} - \frac{C_P^*}{C_P^{0*}}e^{-(1-\alpha)nF\eta/(RT)}\right) \quad (1)$$

Here, j is the current density, j_0^0 is the exchange current density at standard concentration, C_R^* and C_P^* are the actual surface concentrations of chemicals in the catalyst layer, C_R^{0*} and C_P^{0*} are the standard concentrations of reactants and products, α is the charge transfer coefficient, and η is the activation overpotential. In general, in a two-electrode fuel cell using hydrogen–air (or oxygen), cathode activation loss is dominant by the RDS. This is due to the relatively slow reduction reaction, whereas the oxidation of glucose is very difficult and slow, resulting in a very large anode activation loss. In addition, it is well-known from various studies such as experimental data of polarization curves and impedance. A low reactant concentration loss at the interface still occurs at low current densities, first by lowering the thermodynamic Nernst voltage and increasing the activation loss according to the kinetics.[53] Particular circumstances can make the fuel cell
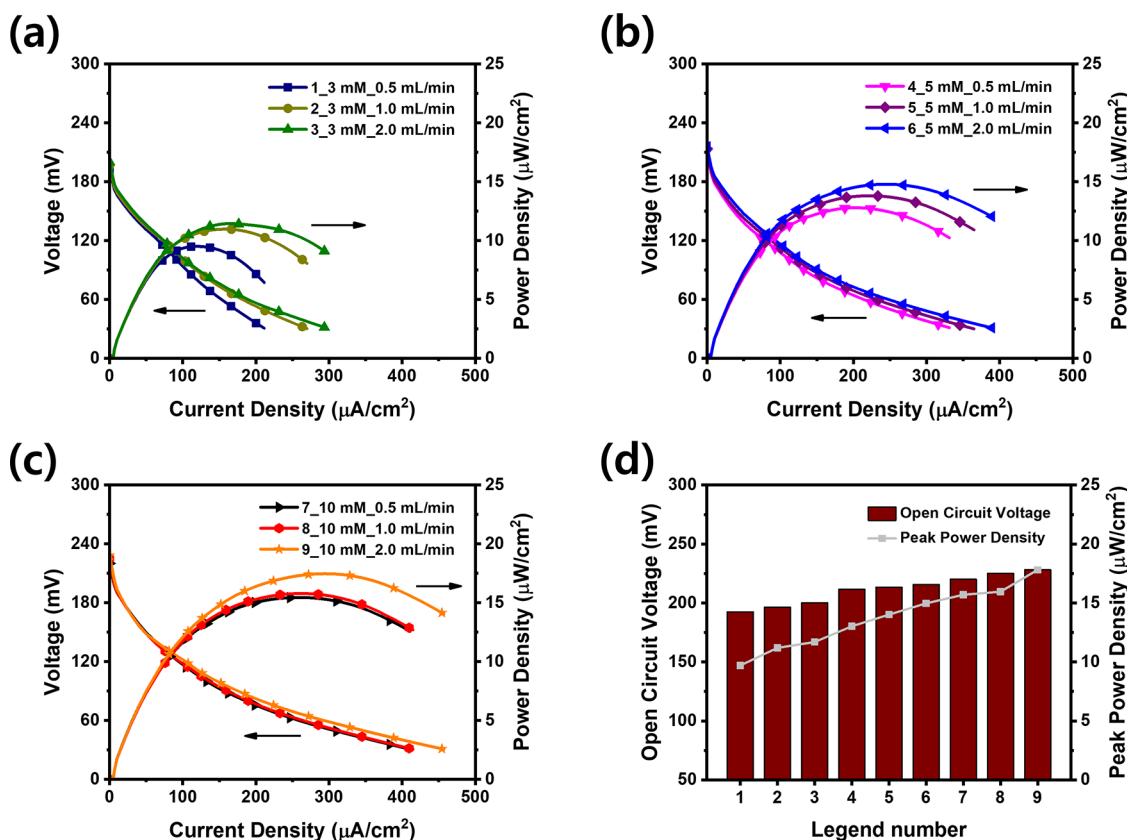

Figure 2. Polarization and performance curves when CP_AA (carbon paper, PTFE nontreatment, and MPL nonexistence) from Table 1 was used as a GDL as the anode side under the following glucose concentration conditions: (a) 3, (b) 5, and (c) 10 mM. (d) Graph of open-circuit voltage and peak power density from (a–c) according to the legend number. As the legend number increases at the same glucose concentration, the flow rate of glucose injected into the inlet of the anode increases from 0.5 to 2.0 mL min^{-1}. The single-cell performance was measured at a temperature of 36.5 °C, and the cathode was supplied with a dry O$_2$ flow rate of 10 sccm.
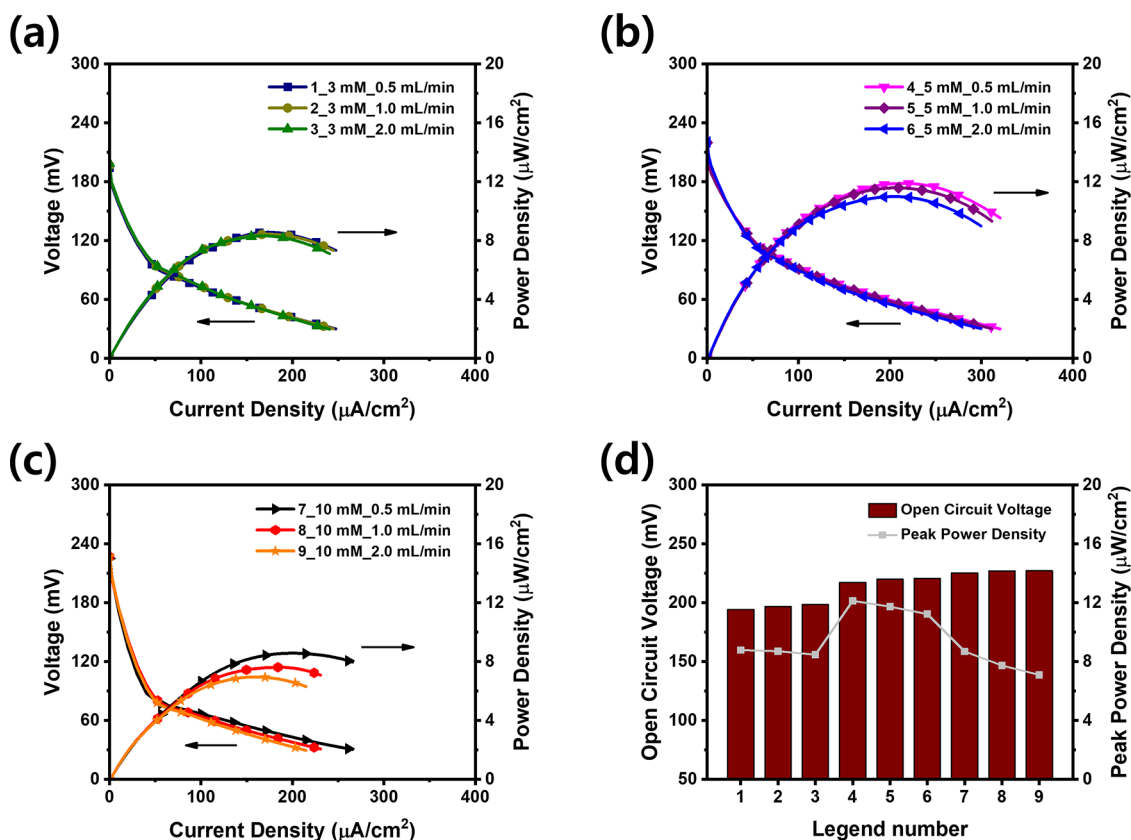
Figure 3. Polarization and performance curves when CP_BA (carbon paper, only PTFE processing) from Table 1 was used as a GDL as the anode side under the following glucose concentration conditions: (a) 3, (b) 5, and (c) 10 mM. (d) Graph of open-circuit voltage and peak power density from (a–c) according to the legend number. As the legend number increases at the same glucose concentration, the flow rate of glucose injected into the inlet of the anode increases from 0.5 to 2.0 mL min^{-1}. The single-cell performance was measured at a temperature of 36.5 °C, and the cathode was supplied with a dry O$_2$ flow rate of 10 sccm.

voltage close to zero due to activation loss before reaching the theoretical limiting current density.[53] As indicated by Figures 2−4, the actual generated current is minimal, showing a polarization curve due to activation loss in the low current density region. To improve this, an appropriate catalyst for enhancing the GOR is required, and the amount of glucose permeating into the anode diffusion layer should be increased. In the end, the OCV and performance depend significantly on the amount of glucose reaching the catalyst. The amount of permeated glucose varies according to the characteristics of the diffusion layer.

Figure 2 shows the polarization curve and power density according to the legend number when CP_AA to the anode and CP_BC to the cathode are applied as diffusion layers. When CP_AA is used for the anode, the performance and OCV increase as the concentration and flow rate of glucose increase. In Figure 2a, when the glucose solution was 3 mM, the peak power density (PPD) increased to 9.70, 11.2, and 11.7 μW cm^{-2} as the glucose flow rate injected into the anode increased from 0.5 to 2.0 mL min^{-1}. At 5 mM, as shown in Figure 2b, the PPD increased to 13.0, 14.0, and 15.0 μW cm^{-2}. It increased to 15.7, 16.0, and 17.8 μW cm^{-2} at 10 mM in Figure 2c. In addition, as the flow rate increases at the same aqueous solution concentration, the current density tends to increase. The current densities at a cutoff voltage of 30 mV were 211, 270, and 294 μA cm^{-2} at 3 mM and 331, 365, and 390 μA cm^{-2} at 5 mM as the glucose flow rate increased from 0.5 to 2.0 mL min^{-1} and 411, 415, and 457 μA cm^{-2} at 10 mM.

Figure 2d shows a graph that summarizes the performance and OCV for the nine cases in Figure 2a−c. The OCV increases to 193, 196, 200, 212, 213, 216, 220, 225, and 228 mV as the flow rate and concentration increase according to the experimental conditions (as the legend number increases). Overall, when CP_AA was applied to the anode side, the higher the concentration and flow rate of the glucose solution, the higher the PPD, maximum current density, and OCV. It suggests that the electrochemical reaction in the catalyst layer occurred directly and rapidly.

To analyze this phenomenon, it is necessary to understand the characteristics of the diffusion layer and to understand fluid behavior in porous media. The concentration of the reactants in the catalyst layer was always lower than the average concentration in the flow path. At a steady state, glucose is transported by diffusion in the diffusion layer by the concentration gradient and is expressed by Fick's law[53] as follows:

$$J_{d,glucose} = -D_{glucose}^{d,eff} \frac{C_{glucose}^* - C_{glucose}^0}{\delta^d} \tag{2}$$

where $J_{d,\,glucose}$ is the glucose flux in the diffusion layer and $D_{glucose}^{d,\,eff}$ is the effective diffusion coefficient of glucose. $C_{glucose}^*$ and $C_{glucose}^0$ are the average reactant concentrations of glucose in the catalyst layer and the flow path, respectively, and δ^d is the thickness of the electrode. The effective diffusion coefficient of glucose is given by Bruggeman's correlation and the calibration equation[54,55] as follows:
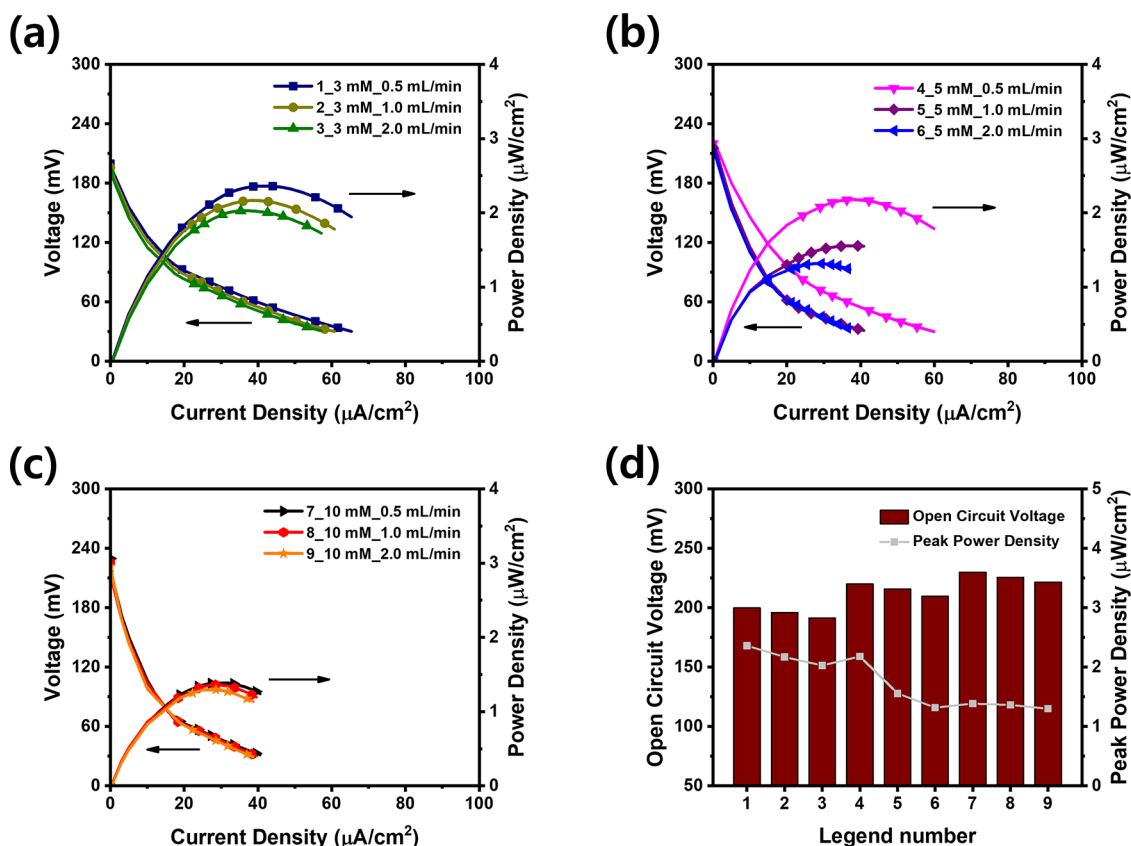
Figure 4. Polarization and performance curves when CP_BC (carbon paper, PTFE processing, and MPL presence) from Table 1 was used as a GDL as the anode side under the following glucose concentration conditions: (a) 3, (b) 5, and (c) 10 mM. (d) Graph of open-circuit voltage and peak power density from (a−c) according to the legend number. As the legend number increases at the same glucose concentration, the flow rate of glucose injected into the inlet of the anode increases from 0.5 to 2.0 mL min^{-1}. The single-cell performance was measured at a temperature of 36.5 °C, and the cathode was supplied with a dry O_2 flow rate of 10 sccm.

$$D_{glucose}^{d,eff} = \varepsilon^\tau D_{glucose}^{d,bulk} \tag{3}$$

Here, $D_{glucose}^{d,bulk}$ is the bulk diffusion coefficient of glucose in the flow path and the electrode boundary layer, ε is the porosity of the diffusion layer, and τ is the tortuosity. Various relational expressions can explain the porosity and tortuosity in porous media. In general, when discussing mass transport within an electrode, it is assumed that the electrode thickness matches the diffusion layer thickness. The diffusion coefficient of bulk glucose is affected by the supplied glucose concentration, temperature and pressure, and molecular weight. The effective diffusion coefficient may be less than the general diffusion coefficient due to the complex structure of the diffusion layer and the porosity, pore size, and tortuosity.

In the properties of the diffusion layer investigated in Table 1, CP_AA showed the highest porosity. When the GDBL was treated with PTFE, as the density increased, the porosity decreased and hydrophobicity increased.[56−58] Therefore, CP_AA has a higher porosity than CP_BA and CP_BC, and according to eqs 2 and 3, the effective diffusion coefficient of glucose increases. In addition, without any treatment, glucose passes more easily through the less hydrophobic diffusion layer. The glucose fuel cell forms an overall low current density, which may be due to the slight concentration gradient due to the insignificant difference between the glucose concentration in the catalyst layer and the flow path. When the permeability of the diffusion layer increases with an increase in the bulk concentration of glucose, the amount of

glucose reacting in the catalyst layer increases, resulting in a faster electrochemical reaction and a tremendous concentration difference. As a result, as the concentration of glucose in the diffusion layer of CP_AA increased, the performance and OCV are improved. The thickness of the diffusion layer used in this experiment is shown in Table 1, and the thickness of CP_AA is the thinnest at 190 μm. With a thicker diffusion layer, the through-plane resistance and the reactant path would increase; thus, it is deemed that the ohmic and mass transport losses could be exacerbated.[59,60] The thinner diffusion layer provides a pathway for the glucose solution to reach the catalyst layer in the through-plane direction as the glucose flow rate increases, leading to a faster GOR. In other words, as the thickness of the diffusion layer decreases according to eq 2, glucose diffusion is increased, which is proportional to the current caused by the electrochemical reaction in the fuel cell, so it is thought to show a higher current density under the same conditions.

A fluid is supplied by convection inside the flow path, and as the glucose flow rate increases, the fluid velocity increases. The flow of this fluid is transmitted to the contact surface of the flow path and the diffusion layer in the horizontal direction. As the horizontal velocity increases, the vertical velocity of the through-plane passing through the diffusion layer increases. When the flow rate of the supplied reactant increases, convection in the flow path mixes with the diffusion layer and penetrates to the inside of the electrode. This reduces the diffusion thickness of the diffusion layer, thus enhancing the

overall permeation.[53] Since the concentration of the glucose solution used in this experiment was extremely low (3 to 10 mM), the total diffusion of glucose can be considered as a Newtonian fluid. At this time, the behavior of a Newtonian fluid in a porous medium can be calculated using Darcy's law,[55] and this equation is as follows:

$$Q = AV^d = A \frac{K_{sat} \Delta P}{\mu \delta^d} \tag{4}$$

where Q is the average flow rate of the supplied fluid, A is the cross-sectional area through which the flow passes, V^d is the average velocity of water in the diffusion layer, K_{sat} is the permeability of water passing through the diffusion layer in a saturated flow, ΔP is the pressure gradient of the diffusion layer, μ is the viscosity of the water, and δ^d is the thickness of the diffusion layer. In this case, water can be considered to contain glucose. Controlling the other variables, increasing the flow rate of the reaction fluid also increases the flow rate and velocity in the direction through the diffusion layer. Therefore, the glucose permeability is increased using eq 4, and more reactants can be supplied to the catalyst layer. A trend of increasing permeability was investigated with an increasing flow rate at the same glucose concentration. In addition, as mentioned earlier, the less hydrophobic and highly porous properties of CP_AA without PTFE and MPL treatment enhanced the permeation of the feed solution, helping glucose to carry out more oxidation reactions in the catalyst layer. When 10 mM glucose was injected into the anode at a flow rate of 2.0 mL min⁻¹, it showed the highest power density among all cases in this experiment. As glucose crossover is remarkably low compared with methanol crossover,[8,21] glucose oxidation at the reaction site dominates the solution passing through the diffusion layer. Therefore, as glucose diffusion increased, the amount consumed at the reaction site of the anode increased, and it was confirmed that the highest power density was exhibited due to the low anodic activation loss. The graphs in Figure 2a−c confirm this, and in the GDBL environment of CP_AA, as the concentration and flow rate of glucose increased, glucose diffusion increased, and the voltage drop from OCV was gradual. As a result, a higher current can be generated, and the best performance is achieved.

In addition to the intrinsic properties of the diffusion layer, electrical conductivity affects the performance of the fuel cell. The electrical conductivity should be as high as possible to minimize ohmic losses by effectively conducting electrons between the catalyst layer and current collectors. The electrical resistivity summarized in Table 1 indicates the diffusion layer resistance in the through-plane direction. In other words, when CP_AA with the smallest electrical resistivity was applied, the electrical conductivity through the collection of electrons was the largest. The performance of the glucose fuel cell increased as the glucose concentration and flow rate were increased by adding various characteristics of the diffusion layer mentioned above.

Effects of Hydrophobicity of Carbon Paper by PTFE Treatment on Glucose Permeability.
Figure 3 shows the polarization curve and power density according to the increase in glucose concentration and flow rate when CP_BA at the anode and CP_BC at the cathode were inserted as diffusion layers, and a single cell was assembled and tested. In this case, the performance decreased, and the OCV increased as the flow rate increased at the same glucose concentration. This is

opposite to the increase in performance when the flow rate is increased at the same glucose concentration when CP_AA is used, and the overall change is insignificant. The PPD, according to each glucose concentration, showed a lower overall performance than that of CP_AA. Specifically, the OCV at 10 mM was the highest. Still, the PPD was the lowest compared to the case of operation at 3 and 5 mM, and the performance at 5 mM showed the best performance at the three glucose concentrations. It is confirmed that CP_BA is more hydrophobic than CP_AA due to PTFE treatment, and at the same time, there was a complicated interaction as the properties of the diffusion layer were changed.

In Figure 3a, when the glucose concentration is 3 mM, the PPD decreases to 8.78, 8.70, and 8.47 $\mu W\ cm^{-2}$ as the glucose flow rate supplied to the anode increases from 0.5 to 2.0 mL min⁻¹. At 5 mM, as shown in Figure 3b, the PPD decreased to 12.1, 11.7, and 11.2 $\mu W\ cm^{-2}$. Similarly, in Figure 3c, it decreased to 8.69, 7.74, and 7.09 $\mu W\ cm^{-2}$ at 10 mM. The current densities at 30 mV were 248, 245, and 241 $\mu A\ cm^{-2}$ at 3 mM when the glucose flow rate increased from 0.5 to 2.0 mL min⁻¹, 321, 312, and 300 $\mu A\ cm^{-2}$ at 5 mM, and 266, 231, and 215 $\mu A\ cm^{-2}$ at 10 mM. In Figure 3d, the OCVs are 194, 197, 199, 217, 220, 221, 225, 226, and 227 mV. At the same concentration, the OCV increased as the flow rate increased (the legend number increased).

At the same glucose concentration, as the flow rate was increased, the performance decreased, and the highest performance was observed at 5 mM. A reversal phenomenon is observed at a concentration lower than 10 mM. Compared with applying CP_AA to the anode diffusion layer, the OCV increase was lower, and the overall performance by concentration was also low. In addition, at 10 mM, the electrochemical reaction decreased in the catalyst layer, according to the decrease in fuel permeability, and a more considerable activation loss appeared. Therefore, it is confirmed that increasing the hydrophobicity through the diffusion layer with PTFE treatment adversely affects the use of a higher concentration of glucose solution in a glucose fuel cell using liquid fuel.

In general, in fuel cells using gas as a reactant, hydrophobic agents such as PTFE are treated in the GDL for better liquid water transport.[61] Since PTFE treatment of the GDL is primarily involved in the transport of water, an appropriate PTFE content is essential. Nevertheless, it has been found that the higher the PTFE content in the GDL, the lower the porosity, thermal conductivity, electrical conductivity, and permeability.[62,63] In particular, permeability can be divided into in-plane and through-plane, which depend on the intrinsic properties of the GDL, such as the PTFE content, density, thickness, and the presence of an MPL.[64−66] The average through-plane and in-plane permeability of gas flow across the GDL was slightly higher for the GDL treated with PTFE than the GDL without treatment at the same thickness.[64]

However, it is confirmed that the diffusion layer treated with PTFE can deteriorate the performance of the fuel cell using liquid fuel. The insignificant increase in the permeability of the GDL in all directions by PTFE when using a gas reactant is offset by the deteriorated properties through PTFE treatment. In particular, through PTFE treatment in the porous medium of the diffusion layer, the material's porosity is reduced, and a more hydrophobic environment is created. As shown in Table 1, CP_BA has a lower porosity and a thicker thickness than CP_AA, and as indicated by eqs 2 and 3, a decrease in the

effective diffusion coefficient and an increase in thickness caused by a reduction in the porosity of the diffusion layer caused a decline in the overall glucose diffusion. As a result, the amount of the glucose reactant reaching the catalyst layer decreases, resulting in a low concentration difference from the bulk solution. The current generated by the electrochemical reaction is inevitably lowered. In addition, as the concentration of glucose increased from low to high, the fluid viscosity increased slightly. These factors combine to prevent the reactant from reaching the catalyst layer. Compared with CP_AA, the viscosity at 10 mM resulted in the lowest performance among the three cases of glucose concentration.

The effect of the hydrophobic environment on the glucose fuel cell was more clearly observed when the flow rate was changed. As the flow rate supplied using eq 4 increases, the permeability in the porous medium should increase, but the hydrophobicity of the diffusion layer pushes the feed solution supplied to the bipolar plates, thereby reducing the permeability. Moreover, the increase in the velocity of the fluid flowing in the horizontal direction prevents the increase in velocity in the vertical direction by hydrophobicity so that mixing by convection into the diffusion layer does not proceed actively. Thus, with a thicker diffusion layer, the amount of glucose solution that undergoes an electrochemical reaction in the catalyst layer decreases, causing a decrease in the overall performance. Additionally, according to the concentration, the improvement of OCV showed a tendency to increase, as did CP_AA. Still, with a lower increase, the increase in hydrophobicity by PTFE treatment slowed down the diffusion of reactants. Therefore, a smaller amount of glucose is transferred to the catalyst layer, and electrons are transferred to the current collector via an electrochemical reaction. Compared to CP_AA, CP_BB exhibits a lower current density due to a slightly higher electrical resistivity. Thus, CP_BA treated with PTFE allowed operation at lower glucose concentrations.

Effects of Hydrophobicity and a Microporous Layer of Carbon Paper on Glucose Permeability. Figure 4 shows the results of the experiments by applying CP_BC as a diffusion layer to the anode and the cathode. As the flow rate increases at each concentration of glucose, both the performance and open-circuit voltage decrease, and, evidently, it shows the lowest performance compared to the previous CP_AA and CP_BA. In the previous results, when the carbon paper was treated with PTFE, the performance tended to decrease as the glucose flow rate increased. In CP_BC with an additional MPL, the OCV drops. Compared with the polarization curves in Figures 2 and 3, a more considerable activation loss occurred, which resulted in a significantly lower PPD. Finally, it is confirmed that the diffusion layer including the MPL in the glucose fuel cell has the most adverse effect.

In Figure 4a, as the glucose flow rate injected into the anode increased from 0.5 to 2.0 mL min^{-1}, the PPD decreased to 2.51, 2.34, and 2.17 μW cm^{-2} when the glucose concentration was 3 mM. At 5 mM, as shown in Figure 4b, the PPD decreased to 2.29, 1.58, and 1.41 μW cm^{-2}. Moreover, it decreased to 1.47, 1.44, and 1.42 μW cm^{-2} at 10 mM, as shown in Figure 4c. The current densities at 30 mV are 65.4, 60.6, and 56.0 μA cm^{-2} at 3 mM when the glucose flow rate increases from 0.5 to 2.0 mL min^{-1}, 59.9, 40.9, and 37.0 μA cm^{-2} at 5 mM, and 40.4, 39.6, and 38.7 μA cm^{-2} at 10 mM. It is confirmed that the amount of current generated was notably low compared with that of CP_AA and CP_BA. In Figure 4d,

the OCVs according to the legend number are 200, 196, 191, 220, 216, 210, 230, 226, and 222 mV, and at the same concentration, it decreases as the flow rate increases.

As shown in Figure 3, using CP_BA as the anode diffusion layer, the performance at 5 mM was the best, but in Figure 4, where CP_BC was applied, the performance at the lowest 3 mM was relatively high among the three glucose concentrations. Also, compared with Figures 2 and 3, it is confirmed that an abrupt activation loss occurs. As the glucose concentration increases, the activation loss increases due to a decreased electrochemical reaction by low permeability. In CP_BA, the diffusion layer with the MPL using CP_BC, along with the low increase in OCV through PTFE treatment, leads to a decrease in OCV.

With coating the MPL on the GDBL already treated with PTFE, the GDL has more hydrophobic properties overall. Therefore, it can be expected that when CP_BA is used as the anode diffusion layer described above, the permeation of the bulk solution is worse in CP_BC in the presence of the MPL and harms the glucose fuel cell. This is because the in-plane permeability of the carbon paper GDL is higher than that of the through-plane.[66] In addition, the permeability of the GDL introduced with the MPL is approximately two times lower than that of the GDBL.[67,68] Ultimately, the MPL acts as a barrier in gas transport, lowering through-plane permeability and promoting in-plane permeability.[64] This tendency creates an environment that is difficult to permeate through the through-plane of the diffusion layer when liquid fuel is used.

The material properties of CP_BC, confirmed in Table 1, support the low performance. The PTFE treatment and the MPL showed the lowest porosity and the thickest thickness. Therefore, according to eqs 2 and 3, the glucose diffusion supplied to the anode decreases, and the permeability decreases, so the amount of the reactant reaching the catalyst layer is significantly lowered. In addition, gluconic acid or unreacted glucose generated in the catalyst layer is released, making it difficult to permeate the entire liquid fuel. Consequently, even if the glucose concentration increases, the concentration difference with the catalyst layer does not occur significantly; thus, the amount of permeation through the diffusion layer does not increase. As a result, the overall performance was significantly lower than those of CP_AA and CP_BA. In CP_BC, the glucose concentration was the highest at 3 mM, and the performance decreased as the concentration increased.

As mentioned earlier, the performance decreased as the flow rate increased in a more hydrophobic environment through PTFE treatment. CP_BC, which is more hydrophobic due to the properties of the GDL, including the MPL, prevents the increase in permeability with an increasing flow rate using eq 4. In addition, the addition of the MPL reduced through-plane permeability and increased in-plane permeability. Thickened, the GDL decreased the amount reaching the catalyst layer as the flux of the glucose reactant increased. The low increase in OCV according to the glucose concentration by PTFE treatment confirmed in Figure 3d shows a marked decrease in Figure 4d with the addition of the MPL. As a result, the OCV and performance decrease with an increasing concentration and flow rate, showing the lowest performance and current density in all cases. Specifically, in CP_BA, when the concentration of glucose was 3 mM, the performance change according to the flow rate change was minimal, whereas, in CP_BC, 10 mM was the least sensitive to the flow rate change.

Owing to the presence of the MPL, the difference in the flow rate is not important when operating at a relatively high concentration. Additionally, the highest electrical resistivity of CP_BC, summarized in Table 1, shows a lower current density in all cases with the lowest permeability of the glucose reactant. Thus, when operating a glucose fuel cell, the presence of hydrophobicity and the MPL caused by PTFE treatment of the diffusion layer deteriorates the performance of the fuel cell and prevents operation at higher glucose concentrations.

Table 2 shows the OCV and PPD when three different GDLs tested in this study were applied to the anode. When

Table 2. Effect of Carbon Paper Properties Used as an Anode Diffusion Layer on Open-Circuit Voltage (OCV) and Peak Power Density (PPD) in a Nonenzymatic Glucose Fuel Cell

| legend number | Anode_GDL | | | | | |
| | CP_AA | | CP_BA | | CP_BC | |
	OCV (mV)	PPD (μW cm^{-2})	OCV (mV)	PPD (μW cm^{-2})	OCV (mV)	PPD (μW cm^{-2})
1	193	9.70	194	8.78	200	2.51
2	196	11.2	197	8.70	196	2.34
3	200	11.7	199	8.47	191	2.17
4	212	13.0	217	12.1	220	2.29
5	213	14.0	220	11.7	216	1.58
6	216	15.0	221	11.2	210	1.41
7	220	15.7	225	8.70	230	1.47
8	225	16.0	226	7.74	226	1.44
9	228	17.8	227	7.09	222	1.42

CP_AA was used as the anode diffusion layer, OCV and PPD increased as the concentration and flow rate of glucose increased. CP_BA showed the best performance when the concentration of glucose was 5 mM, and it decreased at 10 mM. In addition, the increase in OCV according to the concentration increase was smaller than that of CP_AA, and as the flow rate increased, the performance at each concentration decreased. This phenomenon occurs because the diffusion layer is more hydrophobic through PTFE treatment, and the material properties have a bad effect on the glucose fuel cell. When CP_BC was applied, it was opposite to that of CP_AA. At each glucose concentration, the OCV and PPD decreased as the flow rate increased, and the three diffusion layer cases showed the lowest performance. CP_BC with PTFE treatment and the MPL added to the carbon paper-based diffusion layer provides an environment where the glucose reactant does not penetrate more.

Overall, when CP_AA based on carbon paper without any treatment was used, it allowed operation at higher concentrations and flow rates of glucose and showed the best performance. This is considered due to the less hydrophobic properties of CP_AA compared to other diffusion layers, along with high porosity, thin thickness, and low electrical resistivity. Therefore, it is thought that properties close to CP_AA are the most advantageous for operating nonenzymatic glucose fuel cells. Nevertheless, glucose fuel cells with proton exchange membranes (e.g., Nafion) based on hydrogen ion transport eventually crossover during long-term operation. This may be the reason why the intermediates and products are adsorbed on the catalyst surface in the glucose oxidation reaction. Therefore, although the use of a proton exchange membrane

has various advantages in a nonenzymatic glucose fuel cell, the nanostructure needs to be improved.

CONCLUSIONS

Carbon paper was applied as an anode diffusion layer of a nonenzymatic glucose fuel cell to investigate which properties are advantageous for permeability. Three cases were considered: CP_AA based on carbon paper, CP_BA treated with polytetrafluoroethylene (PTFE), and CP_BC with PTFE and a microporous layer (MPL) added. Glucose concentrations were 3, 5, and 10 mM, and flow rates were 0.5, 1.0, and 2.0 mL min^{-1}. As a result, the open-circuit voltage (OCV) and peak power density (PPD) increased as the glucose concentration and flow rate increased. At this time, when 10 mM glucose was injected at 2.0 mL min^{-1}, the performance was the highest, and the PPD was 17.81 μW cm^{-2}, the highest among all of the experimental data. In PTFE-treated CP_BA, the PPD decreased as the flow rate increased at each glucose concentration, and the increase in OCV with an increasing flow rate was low. Moreover, CP_BC with an added MPL showed an opposite trend to that of CP_AA. As the flow rate increased at each concentration, the OCV and PPD decreased, and the performance was the lowest in all cases. Therefore, it is speculated that the introduction of PTFE treatment and the MPL into the diffusion layer adversely affects the performance of the glucose fuel cell.

We confirmed that the properties of the diffusion layer based on untreated carbon paper are advantageous for glucose fuel cells. The OCV and PPD increase as the concentration and flow rate of glucose increase. This implies that it is possible to operate nonenzymatic glucose fuel cells at higher glucose concentrations and flow rates. If the OCV and PPD, according to the change in the concentration and flow rate of glucose injected into the anode inlet, are optimized, then the concentration and flow rate of glucose can be predicted using the acquired data. In addition, in this experiment, a bipolar plate of a single serpentine channel was used. The shape of the bipolar plate of the glucose fuel cell, along with the characteristics of the diffusion layer, affects the permeability of glucose. Thus, future work will focus on optimizing the performance of nonenzymatic glucose fuel cells according to the flow channel shape. Glucose fuel cell operation at low power is still a problem because of the issue of glucose oxidation. However, despite these limitations, the many advantages of glucose will enable its application to various biobased and medical devices.

EXPERIMENTAL SECTION

Fabrication of Membrane Electrolyte Assembly. The membrane electrolyte assembly (MEA) used for the experiments was fabricated as follows: PtRu/C (20 wt % Pt, 10 wt % Ru; Sigma-Aldrich, Inc., USA) and Pt/C (40 wt % Pt; Alfa Aesar, Inc., USA) were used for the anode and cathode sides, respectively. The catalyst loading amount of both electrodes was the same at 1.0 mg cm^{-2}. The catalyst ink consisted of deionized (DI) water, isopropyl alcohol (IPA) (Daejung Chemical Co., Republic of Korea), and Nafion ionomer solution (5 wt %; Sigma-Aldrich, Inc., USA) and was sonicated for 30 min. Nafion 212 (DuPont, Inc., USA) with a thickness of 50.8 μm used as a proton exchange membrane was fixed on a vacuum hot plate and maintained at a surface temperature of 80 °C. A well-dispersed catalyst slurry was applied to the

membrane so that the reaction area was 1.0 cm² through spraying. The catalyst-coated membrane (CCM) prepared in this manner was dried at room temperature for approximately 10 h, and gas diffusion layers (GDLs; SGL Carbon, Ltd., Germany) were placed on the catalyst layer. A carbon paper GDL (Sigracet 29BC, SGL Carbon, Ltd., Germany) containing a polytetrafluoroethylene (PTFE)-treated gas diffusion backing layer (GDBL) and a microporous layer (MPL) was fixed into the cathode. GDLs (29AA, 29BA, and 29BC; SGL Carbon, Ltd., Germany) with a conventional carbon paper GDBL, PTFE treatment, both PTFE and an MPL were prepared as the anode. It was confirmed that a diffusion layer of excellent quality was produced through the manufacturing process and SEM images provided by Sigracet. In addition, properties such as porosity, thickness, and electrical resistivity were investigated for various types according to PTFE treatment and the MPL, which are summarized in Table 1.[51] MEAs were prepared by inserting three different anode GDLs into the catalyst layers symmetrically coated on both sides of the proton exchange membrane.

Configuration of the Glucose Fuel Cell. Figure 5 shows an exploded view of the nonenzymatic glucose fuel cell
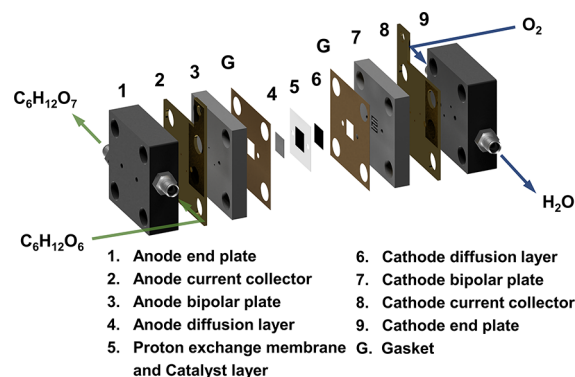

Figure 5. Exploded view of the nonenzymatic glucose fuel cell in this experiment. In configuring the MEA, conventional GDLs (Sigracet 29BC; SGL Carbon, Ltd., Germany) were used with the PTFE-treated GDBL and the MPL on the cathode side diffusion layer, and experiments were conducted on three different cases depending on the presence of the PTFE-treated GDBL and the MPL on the anode side diffusion layer, as shown in Table 1.

fabricated for this experiment. The previously prepared MEA was sandwiched between bipolar plates made of graphite and Teflon gaskets. The thickness of the bipolar plates was 10 mm for both electrodes, and the flow channel (1.5 mm width, 0.5 mm rib, and 1 mm depth) had a single serpentine shape with a reaction area of 1.0 cm². A current collector was prepared on each electrode to move electrons generated in the electrochemical reaction through the catalyst and plated to prevent corrosion. The endplate had a thickness of 20 mm, and four holes for fastening bolts and nuts were machined and insulated. The single-cell assembly was tightened with a uniform force of 6.0 N m for all four bolts using a torque wrench.

Characterization of the Nonenzymatic Glucose Fuel Cell. To proceed with this experiment after manufacturing a single-cell assembly, a glucose solution injected into the anode was prepared as follows: A 50 mL polypropylene Falcon tube was individually filled with 0.01 M phosphate-buffered saline (PBS) solution (pH 7.4, Invitrogen, Inc., Germany) diluted with deionized(DI) water. After adding 3, 5, and 10 mM

glucose granular powder (D-glucose anhydrous, Fisher Scientific, Ltd., United Kingdom), the mixture was sonicated for approximately 1 h. The aqueous solution of glucose prepared in this manner was drawn into a disposable syringe with a capacity of 50 mL, and the flow rate was controlled by a syringe pump (New Era Pump Systems, Inc., USA) and transferred to the anode inlet of the single experimental cell at atmospheric pressure. Table 3 shows the concentration and

Table 3. The Legend Number According to the Concentration and Flow Rate of Glucose Injected into the Anode (Expressed in Figures 2−4)

legend number	glucose concentration (mM)	glucose flow rate (mL min⁻¹)
1	3	0.5
2	3	1.0
3	3	2.0
4	5	0.5
5	5	1.0
6	5	2.0
7	10	0.5
8	10	1.0
9	10	2.0

flow rate of glucose used in this experiment classified by the legend number. The experimental parameters were set to increase the glucose concentration and flow rate in each case. All experimental cases were conducted at ambient pressure while maintaining the cell temperature at 36.5 °C. Dry oxygen was supplied to the cathode at a rate of 10 sccm using a mass flow controller.

Before measuring the performance of nonenzymatic glucose fuel cells, single cells were activated as follows. First, an aqueous solution of glucose and dry oxygen was supplied to the anode and the cathode, respectively, to the assembled single-cell assembly. Then, MEAs were activated at 80 mV for 2 h for stable operation. After that, the glucose concentration was supplied at a constant flow rate from low to high, and it was set to a steady state. When the open-circuit voltage (OCV) was stabilized, the polarization curve showed a sweep rate of 1.0 mV s⁻¹ from a low glucose concentration to an electrochemical workstation (Wonatech Co., Republic of Korea) from OCV to 30 mV by the potentiodynamic method. To measure the effectiveness of the anode diffusion layer on the performance as the glucose concentration and flow rate change, other variables were controlled, and measurements were repeated for stable operation.

■ AUTHOR INFORMATION

Corresponding Author

Taehyun Park − *School of Mechanical Engineering, Soongsil University, Seoul 06978, Republic of Korea;* orcid.org/0000-0002-1270-7703; Phone: +82-2-820-0669; Email: taehyunpark@ssu.ac.kr

Authors

Hyeonjin Cha − *School of Mechanical Engineering, Soongsil University, Seoul 06978, Republic of Korea;* orcid.org/0000-0002-7449-4301

Obeen Kwon − *School of Mechanical Engineering, Soongsil University, Seoul 06978, Republic of Korea*

Jaeyeon Kim − *School of Mechanical Engineering, Soongsil University, Seoul 06978, Republic of Korea*

Heesoo Choi − *School of Mechanical Engineering, Soongsil University, Seoul 06978, Republic of Korea*

Hongnyoung Yoo − *School of Mechanical Engineering, Soongsil University, Seoul 06978, Republic of Korea*

Hyeok Kim − *School of Mechanical Engineering, Soongsil University, Seoul 06978, Republic of Korea*

Complete contact information is available at:
https://pubs.acs.org/10.1021/acsomega.1c05199

Notes
The authors declare no competing financial interest.

■ ABBREVIATIONS

PEM, proton exchange membrane; AEM, anion exchange membrane; GOR, glucose oxidation reaction; ORR, oxygen reduction reaction; PTFE, polytetrafluoroethylene; CCM, catalyst-coated membrane; MEA, membrane electrolyte assembly; GDBL, gas diffusion backing layer; GDL, gas diffusion layer; MPL, microporous layer; OCV, open-circuit voltage; PPD, peak power density

■ REFERENCES

(1) Jeon, W. Y.; Lee, J. H.; Dashnyam, K.; Choi, Y. B.; Kim, T. H.; Lee, H. H.; Kim, H. W.; Kim, H. H. Performance of a Glucose-Reactive Enzyme-Based Biofuel Cell System for Biomedical Applications. *Sci. Rep.* **2019**, *9*, 1.

(2) Slaughter, G.; Kulkarni, T. Detection of Human Plasma Glucose Using a Self-Powered Glucose Biosensor. *Energies* **2019**, *12*, 825.

(3) Xu, Q.; Zhang, F.; Xu, L.; Leung, P.; Yang, C.; Li, H. The Applications and Prospect of Fuel Cells in Medical Field: A Review. *Renewable Sustainable Energy Rev.* **2017**, *67*, 574−580.

(4) Frei, M.; Martin, J.; Kindler, S.; Cristiano, G.; Zengerle, R.; Kerzenmacher, S. Power supply for electronic contact lenses: abiotic glucose fuel cells vs. Mg/Air batteries. *J. Power Sources* **2018**, *401*, 403−414.

(5) Gamella, M.; Koushanpour, A.; Katz, E. Biofuel Cells − Activation of Micro- and Macro-Electronic Devices. *Bioelectrochemistry* **2018**, *119*, 33−42.

(6) Brouzgou, A.; Song, S.; Tsiakaras, P. Carbon-Supported PdSn and Pd₃Sn₂ Anodes for Glucose Electrooxidation in Alkaline Media. *Appl. Catal., B* **2014**, *158-159*, 209−216.

(7) Brouzgou, A.; Yan, L. L.; Song, S. Q.; Tsiakaras, P. Glucose Electrooxidation over PdₓRh/C Electrocatalysts in Alkaline Medium. *Appl. Catal., B* **2014**, *147*, 481−489.

(8) Fujiwara, N.; Yamazaki, S.-I.; Siroma, Z.; Ioroi, T.; Senoh, H.; Yasuda, K. Nonenzymatic Glucose Fuel Cells with an Anion Exchange Membrane as an Electrolyte. *Electrochem. Commun.* **2009**, *11*, 390−392.

(9) Chen, J.; Zhao, C. X.; Zhi, M. M.; Wang, K.; Deng, L.; Xu, G. Alkaline Direct Oxidation Glucose Fuel Cell System Using Silver/Nickel Foams as Electrodes. *Electrochim. Acta* **2012**, *66*, 133−138.

(10) Kerzenmacher, S.; Ducrée, J.; Zengerle, R.; von Stetten, F. Energy Harvesting by Implantable Abiotically Catalyzed Glucose Fuel Cells. *J. Power Sources* **2008**, *182*, 1−17.

(11) Mather, A.; Pollock, C. Glucose Handling by the Kidney. *Kidney Int.* **2011**, *79*, 51−56.

(12) Rubino, R. S.; Gan, H.; Takeuchi, E. S. Implantable Medical Applications of Lithium-Ion Technology. *Proc. Annu. Battery Conf. Appl. Adv.* **2002**, 123−127.

(13) Greatbatch, W.; Lee, J. H.; Mathias, W.; Eldridge, M.; Moser, J. R.; Schneider, A. A. The Solid-State Lithium Battery: A New Improved Chemical Power Source for Implantable Cardiac Pacemakers. *IEEE Trans. Biomed. Eng.* **1971**, *BME-18*, 317−324.

(14) Jeffrey, K.; Parsonnet, V. Cardiac Pacing, 1960-1985: A Quarter Century of Medical and Industrial Innovation. *Circulation* **1998**, *97*, 1978−1991.

(15) Sue, C. Y.; Tsai, N. C. Human Powered MEMS-Based Energy Harvest Devices. *Appl. Energy* **2012**, 390−403.

(16) Oncescu, V.; Erickson, D. High volumetric power density, non-enzymatic, glucose fuel cells. *Sci. Rep.* **2013**, *3*, 1.

(17) Omer, A. E.; Shaker, G.; Safavi-Naeini, S.; Kokabi, H.; Alquié, G.; Deshours, F.; Shubair, R. M. Low-Cost Portable Microwave Sensor for Non-Invasive Monitoring of Blood Glucose Level: Novel Design Utilizing a Four-Cell CSRR Hexagonal Configuration. *Sci. Rep.* **2020**, *10*, 15200.

(18) Shahri, A. A.; Omidvar, A. H.; Rehder, G. P.; Serrano, A. L. C. A High Sensitivity Microwave Glucose Sensor. *Meas. Sci. Technol.* **2021**, *32*, 075104.

(19) Kavanagh, P.; Boland, S.; Jenkins, P.; Leech, D. Performance of a Glucose/O₂ Enzymatic Biofuel Cell Containing a Mediated Melanocarpus Albomyces Laccase Cathode in a Physiological Buffer. *Fuel Cells* **2009**, *9*, 79−84.

(20) Cosnier, S.; le Goff, A.; Holzinger, M. Towards Glucose Biofuel Cells Implanted in Human Body for Powering Artificial Organs: Review. *Electrochem. Commun.* **2014**, *38*, 19−23.

(21) Santiago, Ó.; Navarro, E.; Raso, M. A.; Leo, T. J. Review of Implantable and External Abiotically Catalysed Glucose Fuel Cells and the Differences between Their Membranes and Catalysts. *Appl. Energy* **2016**, *179*, 497−522.

(22) Dector, A.; Escalona-Villalpando, R. A.; Dector, D.; Vallejo-Becerra, V.; Chávez-Ramírez, A. U.; Arriaga, L. G.; Ledesma-García, J. Perspective Use of Direct Human Blood as an Energy Source in Air-Breathing Hybrid Microfluidic Fuel Cells. *J. Power Sources* **2015**, *288*, 70−75.

(23) Katz, E.; MacVittie, K. Implanted biofuel cells operating in vivo—methods, applications and perspectives—feature article. *Energy Environ. Sci.* **2013**, *6*, 2791−2803.

(24) Barelli, L.; Bidini, G.; Calzoni, E.; Cesaretti, A.; di Michele, A.; Emiliani, C.; Gammaitoni, L.; Sisani, E. Enzymatic Fuel Cell Technology for Energy Production from Bio-Sources. *AIP Conf. Proc.* **2019**, *2191*, No. 020014.

(25) Chu, M.; Zhang, Y.; Yang, L.; Tan, Y.; Deng, W.; Ma, M.; Su, X.; Xie, Q.; Yao, S. A Compartment-Less Nonenzymatic Glucose-Air Fuel Cell with Nitrogen-Doped Mesoporous Carbons and Au Nanowires as Catalysts. *Energy Environ. Sci.* **2013**, *6*, 3600−3604.

(26) de Sá, M. H.; Brandão, L. Non-Enzymatic Direct Glucose Fuel Cells (DGFC): A Novel Principle towards Autonomous Electrochemical Biosensors. *Int. J. Hydrogen Energy* **2020**, *45*, 29749−29762.

(27) An, L.; Zhao, T. S.; Shen, S. Y.; Wu, Q. X.; Chen, R. Alkaline Direct Oxidation Fuel Cell with Non-Platinum Catalysts Capable of Converting Glucose to Electricity at High Power Output. *J. Power Sources* **2011**, *196*, 186−190.

(28) Khoobi, A.; Salavati-Niasari, M. High Performance of Electrocatalytic Oxidation in Direct Glucose Fuel Cell Using Molybdate Nanostructures Synthesized by Microwave-Assisted Method. *Energy* **2019**, *178*, 50−56.

(29) Song, B. Y.; He, Y.; He, Y. L.; Huang, D.; Zhang, Y. W. Experimental Study on Anode Components Optimization for Direct Glucose Fuel Cells. *Energy* **2019**, *176*, 15−22.

(30) Rapoport, B. I.; Kedzierski, J. T.; Sarpeshkar, R. A Glucose Fuel Cell for Implantable Brain-Machine Interfaces. *PLoS One* **2012**, *7*, No. e38436.

(31) Ishimoto, T.; Kazuno, H.; Kishida, T.; Koyama, M. Theoretical Study on Oxidation Reaction Mechanism on Au Catalyst in Direct Alkaline Fuel Cell. *Solid State Ionics* **2014**, *262*, 328−331.

(32) Guerra-Balcázar, M.; Morales-Acosta, D.; Castaneda, F.; Ledesma-García, J.; Arriaga, L. G. Synthesis of Au/C and Au/Pani for Anode Electrodes in Glucose Microfluidic Fuel Cell. *Electrochem. Commun.* **2010**, *12*, 864−867.

(33) Basu, D.; Basu, S. Performance Studies of Pd-Pt and Pt-Pd-Au Catalyst for Electro-Oxidation of Glucose in Direct Glucose Fuel Cell. *Int. J. Hydrogen Energy* **2012**, *37*, 4678−4684.

(34) Meng, L.; Jin, J.; Yang, G.; Lu, T.; Zhang, H.; Cai, C. Nonenzymatic Electrochemical Detection of Glucose Based on Palladium-Single-Walled Carbon Nanotube Hybrid Nanostructures. *Anal. Chem.* **2009**, *81*, 7271−7280.

(35) Luo, D.; Wu, L.; Zhi, J. Fabrication of Boron-Doped Diamond Nanorod Forest Electrodes and Their Application in Nonenzymatic Amperometric Glucose Biosensing. *ACS Nano* **2009**, *3*, 2121−2128.

(36) Kerzenmacher, S.; Ducrée, J.; Zengerle, R.; von Stetten, F. An Abiotically Catalyzed Glucose Fuel Cell for Powering Medical Implants: Reconstructed Manufacturing Protocol and Analysis of Performance. *J. Power Sources* **2008**, *182*, 66−75.

(37) Prilutsky, S.; Schechner, P.; Bubis, E.; Makarov, V.; Zussman, E.; Cohen, Y. Anodes for Glucose Fuel Cells Based on Carbonized Nanofibers with Embedded Carbon Nanotubes. *Electrochim. Acta* **2010**, *55*, 3694−3702.

(38) Basu, D.; Basu, S. Synthesis, Characterization and Application of Platinum Based Bi-Metallic Catalysts for Direct Glucose Alkaline Fuel Cell. *Electrochim. Acta* **2011**, *56*, 6106−6113.

(39) Jin, C.; Taniguchi, I. Electrocatalytic Activity of Silver Modified Gold Film for Glucose Oxidation and Its Potential Application to Fuel Cells. *Mater. Lett.* **2007**, *61*, 2365−2367.

(40) Biella, S.; Prati, L.; Rossi, M. Selective Oxidation of D-Glucose on Gold Catalyst. *J. Catal.* **2002**, *206*, 242−247.

(41) Tominaga, M.; Nagashima, M.; Nishiyama, K.; Taniguchi, I. Surface Poisoning during Electrocatalytic Monosaccharide Oxidation Reactions at Gold Electrodes in Alkaline Medium. *Electrochem. Commun.* **2007**, *9*, 1892−1898.

(42) Huang, W.; Wang, M.; Zheng, J.; Li, Z. Facile Fabrication of Multifunctional Three-Dimensional Hierarchical Porous Gold Films via Surface Rebuilding. *J. Phys. Chem. C* **2009**, *113*, 1800−1805.

(43) Chen, C. C.; Lin, C. L.; Chen, L. C. A Binary Palladium-Bismuth Nanocatalyst with High Activity and Stability for Alkaline Glucose Electrooxidation. *J. Power Sources* **2015**, *287*, 323−333.

(44) Jiang, T.; Yan, L.; Meng, Y.; Xiao, M.; Wu, Z.; Tsiakaras, P.; Song, S. Glucose Electrooxidation in Alkaline Medium: Performance Enhancement of PdAu/C Synthesized by NH3 Modified Pulse Microwave Assisted Polyol Method. *Appl. Catal., B* **2015**, *162*, 275−281.

(45) Li, Y.; Lv, J.; He, Y. A Monolithic Carbon Foam-Supported Pd-Based Catalyst towards Ethanol Electro-Oxidation in Alkaline Media. *J. Electrochem. Soc.* **2016**, *163*, F424−F427.

(46) Li, Y. S.; Zhao, T. S.; Xu, J. B.; Shen, S. Y.; Yang, W. W. Effect of Cathode Micro-Porous Layer on Performance of Anion-Exchange Membrane Direct Ethanol Fuel Cells. *J. Power Sources* **2011**, *196*, 1802−1807.

(47) Huang, J.; Simons, P.; Sunada, Y.; Rupp, J. L. M.; Yagi, S. Pt-Catalyzed D-Glucose Oxidation Reactions for Glucose Fuel Cells. *J. Electrochem. Soc.* **2021**, *168*, No. 064511.

(48) Oncescu, V.; Erickson, D. A Microfabricated Low Cost Enzyme-Free Glucose Fuel Cell for Powering Low-Power Implantable Devices. *J. Power Sources* **2011**, *196*, 9169−9175.

(49) Torigoe, K.; Takahashi, M.; Tsuchiya, K.; Iwabata, K.; Ichihashi, T.; Sakaguchi, K.; Sugawara, F.; Abe, M. High-Power Abiotic Direct Glucose Fuel Cell Using a Gold-Platinum Bimetallic Anode Catalyst. *ACS Omega* **2018**, *3*, 18323−18333.

(50) Basu, D.; Sood, S.; Basu, S. Performance Comparison of Pt-Au/C and Pt-Bi/C Anode Catalysts in Batch and Continuous Direct Glucose Alkaline Fuel Cell. *Chem. Eng. J.* **2013**, *228*, 867−870.

(51) Schweiss, R.; Meiser, C.; Damjanovic, T.; Galbati, I.; Haak, N. SIGRACET gas diffusion layers for PEM fuel cells, electrolyzers and batteries. *SGL GROUP*. https://www.fuelcellstore.com/spec-sheets/sigracet-gdl-white-paper-new-generation.pdf.

(52) Xu, H. Experimental Measurement of Mass Transport Parameters of Gas Diffusion Layer and Catalyst Layer in PEM Fuel Cell, University of Alberta Master's Thesis 2019, DOI: 10.7939/r3-r15v-ef66.

(53) O'hayre, R.; Cha, S.-W.; Colella, W.; Prinz, F. B. *Fuel Cell Fundamentals*; John Wiley & Sons, 2016, DOI: 10.1002/9781119191766.

(54) Baschuk, J. J.; Li, X. Modelling of Polymer Electrolyte Membrane Fuel Cells with Variable Degrees of Water Flooding. *J. Power Sources* **2000**, *86*, 181−196.

(55) Pathak, R.; Basu, S. Mathematical Modeling and Experimental Verification of Direct Glucose Anion Exchange Membrane Fuel Cell. *Electrochim. Acta* **2013**, *113*, 42−53.

(56) El-Kharouf, A.; Mason, T. J.; Brett, D. J. L.; Pollet, B. G. Ex-Situ Characterisation of Gas Diffusion Layers for Proton Exchange Membrane Fuel Cells. *J. Power Sources* **2012**, *218*, 393−404.

(57) Maslan, N. H.; Gau, M. M.; Masdar, M. S.; Rosli, M. I. Simulation of porosity and PTFE content in gas diffusion layer on proton exchange membrane fuel cell performance. *J. Eng. Sci. Technol.* **2016**, *11*, 85−95. https://api.semanticscholar.org/CorpusID:54198710

(58) Wei, J.; Ning, F.; Bai, C.; Zhang, T.; Lu, G.; Wang, H.; Li, Y.; Shen, Y.; Fu, X.; Li, Q.; Jin, H.; Zhou, X. An Ultra-Thin, Flexible, Low-Cost and Scalable Gas Diffusion Layer Composed of Carbon Nanotubes for High-Performance Fuel Cells. *J. Mater. Chem. A* **2020**, *8*, 5986−5994.

(59) Truong, V. M.; Duong, N. B.; Yang, H. Effect of Gas Diffusion Layer Thickness on the Performance of Anion Exchange Membrane Fuel Cells. *Processes* **2021**, *9*, 718.

(60) Lin, G.; van Nguyen, T. Effect of Thickness and Hydrophobic Polymer Content of the Gas Diffusion Layer on Electrode Flooding Level in a PEMFC. *J. Electrochem. Soc.* **2005**, *152*, A1942.

(61) Mortazavi, M.; Tajiri, K. Effect of the PTFE Content in the Gas Diffusion Layer on Water Transport in Polymer Electrolyte Fuel Cells (PEFCs). *J. Power Sources* **2014**, *245*, 236−244.

(62) Lobato, J.; Cañizares, P.; Rodrigo, M. A.; Ruiz-López, C.; Linares, J. J. Influence of the Teflon Loading in the Gas Diffusion Layer of PBI-Based PEM Fuel Cells. *J. Appl. Electrochem.* **2008**, *38*, 793−802.

(63) Burheim, O. S.; Pharoah, J. G.; Lampert, H.; Vie, P. J. S.; Kjelstrup, S. Through-Plane Thermal Conductivity of PEMFC Porous Transport Layers. *J. Fuel Cell Sci. Technol.* **2011**, *8*, DOI: 10.1115/1.4002403.

(64) Mukherjee, M.; Bonnet, C.; Lapicque, F. Estimation of Through-Plane and in-Plane Gas Permeability across Gas Diffusion Layers (GDLs): Comparison with Equivalent Permeability in Bipolar Plates and Relation to Fuel Cell Performance. *Int. J. Hydrogen Energy* **2020**, *45*, 13428−13440.

(65) Tamayol, A.; Bahrami, M. Water Permeation through Gas Diffusion Layers of Proton Exchange Membrane Fuel Cells. *J. Power Sources* **2011**, *196*, 6356−6361.

(66) Gostick, J. T.; Fowler, M. W.; Pritzker, M. D.; Ioannidis, M. A.; Behra, L. M. In-Plane and through-Plane Gas Permeability of Carbon Fiber Electrode Backing Layers. *J. Power Sources* **2006**, *162*, 228−238.

(67) Orogbemi, O. M.; Ingham, D. B.; Ismail, M. S.; Hughes, K. J.; Ma, L.; Pourkashanian, M. Through-Plane Gas Permeability of Gas Diffusion Layers and Microporous Layer: Effects of Carbon Loading and Sintering. *J. Energy Inst.* **2018**, *91*, 270−278.

(68) Ismail, M. S.; Borman, D.; Damjanovic, T.; Ingham, D. B.; Pourkashanian, M. On the Through-Plane Permeability of Microporous Layer-Coated Gas Diffusion Layers Used in Proton Exchange Membrane Fuel Cells. *Int. J. Hydrogen Energy* **2011**, *36*, 10392−10402.